Thermochimica Acta 514 (2011) 67–73

Contents lists available at ScienceDirect

Thermochimica Acta

journal homepage: www.elsevier.com/locate/tca

Kinetics of oxidation of boron powder

Ashish Jain [a], Kitheri Joseph [a], S. Anthonysamy [a,*], G.S. Gupta [b]

[a] Chemistry Group, Indira Gandhi Centre for Atomic Research, Kalpakkam 603102, India
[b] Department of Materials Engineering, Indian Institute of Science, Bangalore 560 012, India

ARTICLE INFO

Article history:
Received 17 June 2010
Received in revised form 1 October 2010
Accepted 13 December 2010
Available online 21 December 2010

Keywords:
Boron
Kinetics
Oxidation
Isoconversional method

ABSTRACT

The kinetics of the oxidation of electrodeposited boron powder and the boron powder produced by the reduction process were studied using thermogravimetry (TG). The oxidation was carried out by heating boron powder in a stream of oxygen. Both isothermal and non-isothermal methods were used to study the kinetics. Model-free isoconversional method was used to derive the kinetics parameters. A two step oxidation reaction (exothermic) was observed. The oxidation reaction could not be completed due to the formation of glassy layer of boric oxide on the surface of boron powder which acts as a barrier for further diffusion of oxygen into the particle. The activation energy obtained using model-free method for electrodeposited boron is 122 ± 7 kJ mol^{-1} whereas a value of 205 ± 9 kJ mol^{-1} was obtained for boron produced by the reduction process (commercially procured boron). Mechanistic interpretation of the oxidation reaction was done using model based method. The activation energy was found to depend on the size distribution of the particles and specific surface area of the powder.

1. Introduction

Boron carbide, containing boron enriched in ^{10}B isotope ($^{10}B \sim 65$ at %) will be used as control rod material in India's first proto type fast breeder reactor (PFBR) [1]. High density pellets of boron carbide containing enriched ^{10}B are produced by a high temperature reaction between the enriched elemental boron and carbon. A pilot plant was established in our laboratory for the production of enriched elemental boron. In this facility boron is electrodeposited on mild steel cathode by molten salt electrolysis of a mixture of potassium chloride, potassium fluoride and potassium tetra fluoroborate. The details of the production of elemental boron and boron carbide are described elsewhere [2,3].

Information on the mechanism and kinetics of the oxidation of elemental boron are required for establishing a procedure for the safe handling of elemental boron in air. Boron undergoes oxidation to form boric oxide by the following reaction: $4B + 3O_2 = 2B_2O_3$. B_2O_3 is a thermodynamically stable compound as it has large negative Gibbs energy of formation (for example, -1139.18 kJ mol^{-1} at 500 K).

Rizzo [4] has studied the oxidation of boron powder compacts (crystalline and amorphous) at temperature between 673 K and 1573 K and reported the formation of a protective coating of boric oxide which broke beyond 1273 K. They have also observed that the oxidation of boron followed a parabolic rate law during the initial stages of the oxidation. However, these authors did not study the mechanistic aspects and kinetics parameters of the oxidation process.

Talley [5] has studied the oxidation of boron in 1 atm pressure of oxygen at 1500–2300 K and observed two rate-limiting processes. They obtained an activation energy of 50 kJ mol^{-1} for the lower temperature region (700–800 K), where the flow of molten B_2O_3 (melting point 723.15 K, formed during the oxidation of boron) is the rate-limiting process, and an activation energy of 321 kJ mol^{-1} for the high temperature region (~2300 K), where evaporation of B_2O_3 is the rate controlling mechanism.

DiGiuseppe and Davidovits [6] have studied the gas phase reactions of boron atoms with O_2, SO_2, CO_2 and N_2O in a flow tube apparatus. They obtained a bimolecular rate constant for the oxidation of boron in oxygen at 300 K by measuring the density of boron in the downstream of flow tube as a function of gas reactant concentration.

In order to explain the reaction of oxygen with the boron beneath the oxide layer Glassman et al. [7] have presented a theoretical explanation and showed that the first stage combustion of the boron takes place by the diffusion of boron through the oxide layer to the B_2O_3–gas interface. Yeh and Kuo [8] observed using environment scanning electron microscopy (ESEM) that at elevated temperatures (>1200 K) the diffusion of boron into molten B_2O_3 (l) dominates over the diffusion of gaseous O_2 through the B_2O_3 (l) layer.

King et al. [9–12] have developed models to describe the mechanism of boron oxidation and combustion. They have assumed that oxygen diffuses through the oxide layer to reach the B–B_2O_3 inter-

* Corresponding author. Tel.: +91 44 27480500x24149; fax: +91 44 27480065.
E-mail address: sas@igcar.gov.in (S. Anthonysamy).

0040-6031/$ – see front matter © 2010 Elsevier B.V. All rights reserved.
doi:10.1016/j.tca.2010.12.004

Table 1
The physicochemical characteristics of the boron samples.

Nature of the sample	Chemical purity (wt%)	Specific surface area (m^2/g)	Particles size (μm)	Bulk density ($g\,cm^{-3}$)
Electrodeposited boron	~96	4.2	<10	0.41
Boron-commercial	~99	3.8	<100	0.45

face. The heterogeneous reaction between oxygen and boron can provide heat for vaporization of the oxide layer. The particle temperature will continue to rise if the heat input is greater than the energy loss associated with vaporization of B_2O_3. If it continues to the point at which the remaining oxide layer is sufficiently thin, an abrupt increase in temperature would take place.

Macek and Semple [13] have observed that the burning time of the boron powder was inversely proportional to the mole fraction of oxygen and ambient gas temperature. This implies that both chemical kinetics and oxidizer diffusion play important role in the bare boron combustion.

Most of the studies reported in the literature describe the high temperature oxidation of boron powder as it is used as combustible in aerospace applications [14]. The information on the quantitative treatment of the data to obtain kinetic parameters (rate constant and activation energy) and mechanistic aspects is scarce. In view of the above it was decided to carry out studies on the oxidation of boron powder. This paper describes isothermal and non isothermal kinetics of the oxidation of elemental boron powder. Oxidation behavior of the electrodeposited boron and boron powder procured commercially (which was synthesized by the reduction of boron halide in the presence of hot tantalum filament henceforth called 'boron-commercial') was studied and kinetic parameters such as activation energy were calculated using isoconversional method. The mechanism of oxidation process is proposed based on the analysis of thermogravimetric data using reported models of the solid state reactions.

2. Experimental

2.1. Chemicals

Boron-commercial (purity >99.999 wt%) was procured from M/s. Aldrich Chemical Company, Inc., USA. Electrodeposited elemental boron (purity >96 wt%) was obtained from the Boron Chemistry Laboratory, Indira Gandhi Centre for Atomic Research, Kalpakkam.

2.2. Experimental procedure

The boron powders were characterized for their chemical composition, impurity content, bulk density, specific surface area, particle size distribution and X-ray diffraction. The boron samples were analyzed for their impurity content by inductively coupled plasma mass spectrometry (ICPMS, Model: Elan 250, M/s. Sciex, Toronto, Canada). The carbon content was determined by oxidizing the sample in a stream of oxygen in an induction furnace and measuring the carbon dioxide evolved by an infrared detector. The X-ray powder patterns were obtained using an X-ray diffractometer (XPERT MPD system obtained from M/s. Philips, The Netherlands), employing filtered Cu Kα radiation. BET surface area of the powder was measured using a continuous flow Nelson Eggersten type surface area analyzer, M/s. Quantasorb Jr. system obtained from Quantachrome, USA. The particle size analysis was carried out with a Mastersizer Particle size analyzer obtained from M/s. Malvern, Worcestershire, UK. The simultaneous thermogravimetry and differential thermal analyses were carried out using a TGA/SDTA851e thermogravimetric analyzer supplied by M/s. Mettler Toledo, Switzerland.

The temperature calibration of thermogravimetric analyzer was carried out by the method of fixed melting points employing International Confederation for Thermal Analysis and Calorimetry (ICTAC) recommended standards such as indium, tin and gold. This equipment has a weight sensitivity of 0.1 μg and a temperature sensitivity of 0.01 K. A Platinum crucible of 70 μl capacity was used as the sample container. For each experiment 5 mg of the boron powder was used as sample. The temperature was measured using a Pt–Pt–10% Rh thermocouple which was in firm contact with the sample holder on which the Pt sample container was placed. The inner muffle of the furnace was constantly purged with oxygen, the flow of which was controlled by a mass flow controller. A constant gas flow of $0.33\,l\,s^{-1}$ and a predetermined rate of heating were used to carry out dynamic experiments. A program with three segments was used for this study. In the first segment the sample was heated from 303 K to 393 K at a heating rate of $10\,K\,min^{-1}$. In the second segment, in order to remove the moisture absorbed on the surface of fine powder, the sample was heated at 393 K for 30 min. In the third segment dynamic experiments were carried out. In this segment sample was heated from 393 K to 1073 K at various heating rates viz. 1, 3, 5, 10 and $15\,K\,min^{-1}$. A fresh sample was taken for each experiment. Reproducibility of the results obtained from different measurements was verified by carrying out measurements in duplicate or triplicate. The results were found to be in excellent agreement with each other. Isothermal experiments were carried out by heating the sample at pre-determined temperatures viz. 713 K, 733 K, 753 K, 773 K, 793 K and 813 K for 420 min. The furnace was preheated to the desired temperature and sample was introduced at that temperature.

3. Results and discussion

The physicochemical properties of the boron powder samples (electrodeposited boron and boron-commercial used in the present study) such as chemical purity, specific surface area, particle size and bulk density are given in Table 1. The total metallic impurities present in the sample were less than 1% (by weight). The detailed chemical assay of electrodeposited boron is described elsewhere [15]. Hence, the influence of metallic impurities on the oxidation behavior of boron is expected to be insignificant. The X-ray diffraction pattern of the electrodeposited boron and boron-commercial is shown in Fig. 1. The X-ray diffraction pattern shows the crystalline nature of boron-commercial. It was observed that the peak positions of the diffraction pattern of boron-commercial match with the standard pattern of rhombohedral boron (JCPDS file no. 80-0322). The X-ray diffraction pattern of electrodeposited boron is also shown in the same figure. The absence of sharp peaks in the diffraction pattern shows the amorphous nature of the electrodeposited boron. This was further confirmed by transmission electron microscopy analysis of the electrodeposited boron where nano crystallites of boron (rhombohedral) were seen embedded in an amorphous mass of boron [16]. The product of oxidation reaction was found to be boric oxide as confirmed by taking X-ray diffraction pattern of the reaction product. The X-ray diffraction pattern matches with the reported pattern for cubic boric oxide JCPDS file no. 06 0297. This X-ray diffraction pattern was recorded after heat treating the oxidized product at 700 K for 150 h in air to convert amorphous boric oxide to crystalline form.

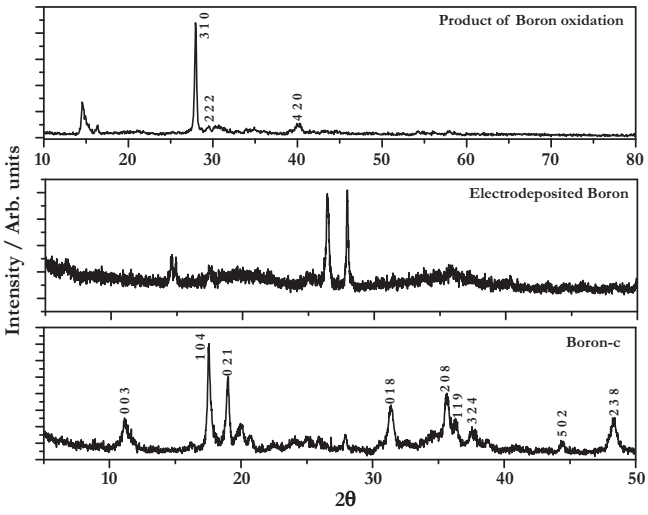

Fig. 1. XRD pattern of boron powders and oxidized product.

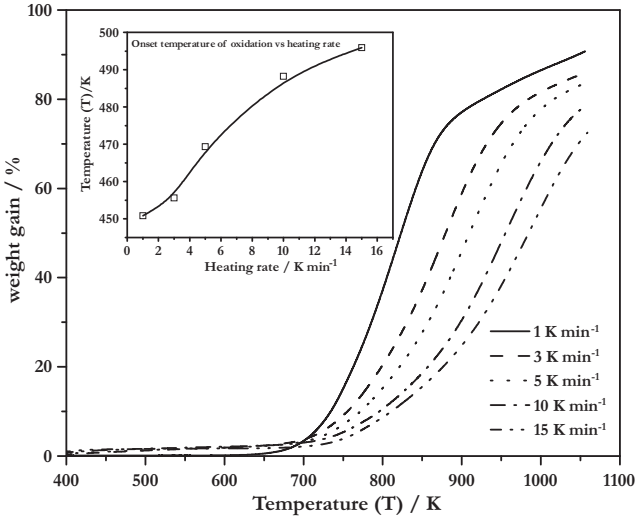

Fig. 3. A plot of percent weight gain as a function of temperature at various heating rates for electrodeposited boron. A plot of the onset temperature as function of heating rate is shown as an inset.

3.1. Oxidation of boron powder

Typical thermal analysis curves [thermogravimetry (TG), derivative thermogravimetry (DTG), differential thermal analysis (DTA)] and sample temperature vs. time curve for the oxidation of electrodeposited boron powder are shown in Fig. 2. Similar curves were obtained for the oxidation of boron-commercial also. The sample was heated from 393 K to 1073 K in the flowing stream of oxygen gas at a heating rate of 5 K min^{-1}. The TGA curve shown in Fig. 2a clearly indicates that there was no measurable weight gain up to 700 K, beyond which a sudden increase in weight due to the oxidation of boron powder is observed. This is reflected as sharp gain in weight in the TGA curve. The weight gain due to oxidation process continued to increase rapidly till temperature reaches 900 K. At temperatures above 900 K, the oxidation was found to be very sluggish as observed as slow rate of increase in weight with temperature. From the TGA curve, it is also clear that the observed weight gain is only ~80–90% and the theoretical weight gain (111 wt% per mol of boron, weight gain calculated from the balanced chemical reaction $4B + 3O_2 = 2B_2O_3$) was not achieved in the temperature range of the present study. Though the thermogravimetry curve (Fig. 2a) shows a single plateau which is indicative of single step oxidation reaction yet derivative thermogravimetry curve (Fig. 2b, shown as inset) shows that the oxidation reaction is not a single step process but a two step process. The rate of oxidation is slow till 730 K and later rapid oxidation of the boron is observed which involve ignition reaction also. The exothermic peak (Fig. 2c) obtained in the DTA curve and the sample temperature vs. time curve (Fig. 2d) shows the exothermic nature of the process. With the help of coupled EGA (Evolved gas analysis) technique, it was confirmed that there was no loss in weight due to vaporization of B_2O_3 (molecular weight ~69.6 g) formed during the oxidation of boron under experimental conditions. As theoretical weight gain was not achieved in the present study, for the convenience of calculation, the weight obtained after the completion of the thermogravimetry experiment was taken as the final weight gain 'w_T' for the oxidation reaction and the fraction of the boron oxidized 'α', was evaluated by the relation

$$\alpha = \frac{w_t - w_i}{w_T - w_i} \quad (1)$$

where w_i, w_T and w_t weights correspond to initial, final and intermediate weight, respectively.

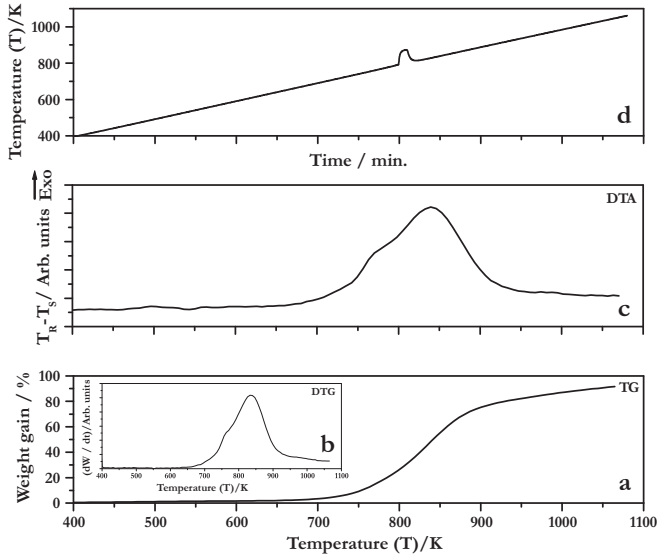

Fig. 2. Thermal analysis curves for the oxidation of electrodeposited boron powder. (a) Thermogravimetry curve, (b) derivative thermogravimetry curve, (c) differential thermal analysis curve, and (d) temperature vs. time curve.

3.2. Kinetic analysis of electrodeposited boron powder using isoconversional method

3.2.1. Non isothermal kinetics

The variation of percentage gain in weight with temperature of oxidation of electrodeposited boron powder at various heating rates is shown in Fig. 3. The curve for electrodeposited boron indicates that the observed weight gain is dependent on the rate of heating. A weight gain of ~90% was observed when boron powder was heated at a rate of 1 K min^{-1} while ~72% weight gain was observed when sample was heated at 15 K min^{-1}. Theoretical weight gain was not achieved in the temperature range and heating rate employed in the present study. This indicates that the reaction products formed during the oxidation reaction had a retarding effect on the progress of the oxidation reaction. The percentage weight gain is higher for lower heating rate and vice versa. This is due to better equilibration of the sample with temperature at lower heating rates. The variation of onset temperature of oxidation with heating rate is shown as an inset in Fig. 3. This shows that

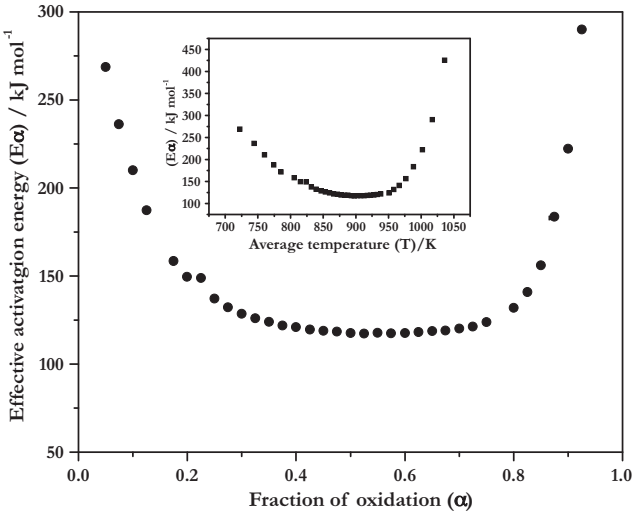

Fig. 4. A plot of E_α as a function of α for electrodeposited boron powder. A plot of E_α as a function of average temperature is shown as an inset.

onset temperature of oxidation reaction increases with increase in heating rate.

The rate of any heterogeneous reaction under non-isothermal condition can be expressed as [17].

$$\frac{d\alpha}{dT} = \frac{k(T)}{\beta} f(\alpha) \tag{2}$$

where α is the fraction of oxidation or degree of conversion at temperature T, $f(\alpha)$ is the conversion function which is dependent on the mechanism of the reaction, β is the rate of heating and $k(T)$ is the temperature dependent Arrhenius rate constant. The integral form of Eq. (2) can be expressed as:

$$g(\alpha) \cong \int_0^\alpha \frac{d(\alpha)}{f(\alpha)} = \int_0^T \frac{A}{\beta} \exp\left[\frac{-E_a}{RT}\right] dT \tag{3}$$

where $g(\alpha)$ is the integral form of $f(\alpha)$, 'A' the pre-exponential factor, 'E_a' the activation energy of reaction and 'R' is the gas constant. From the TGA curve, the fraction oxidized, α, was evaluated by applying Eq. (1).

The effect of temperature (due to change in heating rate) on the activation energy can be obtained by model free isoconversional methods like Kissinger–Akahir–Sunose (KAS) [18,19], which takes the form:

$$\ln \frac{\beta_i}{T_{\alpha,i}^2} = \text{const} - \frac{E_\alpha}{RT_{\alpha,i}} \tag{4}$$

where the subscript 'i' denotes the various heating rates. The slope of the plot $\ln(\beta_i/T_{\alpha,i}^2)$ vs. $1/T_{\alpha,i}$ gives the value of the effective activation energy E_α. The plot of E_α as a function of α is shown in Fig. 4. The variation of effective activation energy, E_α with α can be divided into three regions. For the first region α = 0–0.2, the E_α falls with α. For the second region α = 0.2–0.8, E_α remains constant and for the third region α = 0.8–1 E_α increases with α. The change of E_α with average temperature is shown as an inset in Fig. 4. The decrease in the value of E_α with temperature (up to α = 0.2) indicates that the oxidation rate increases with increasing temperature. The oxidation process of electrodeposited boron consists of formation of B_2O_3 nuclei, growth of nuclei and diffusion of oxygen through the B_2O_3 layer. During the initial stage of oxidation, the process is dominated by both nucleation and growth of B_2O_3 phase (formation of B_2O_3) [19,20]. Hence the activation energy decreases with the fraction oxidized as well as with temperature. For α = 0.2–0.8, the activation energy remains almost constant which indicates that competing processes such as nucleation, growth, sintering, contracting area and volume which may have different activation energy and the effective activation energy does not change with temperature and α. The complex nature of the mechanism of oxidation can be sorted out only by model fit approach. Beyond this α value, the activation energy increases with α, which indicates that there are parallel reactions occurring during oxidation. These parallel reactions could be diffusion of oxygen through the product layer, sintering along with crystallization of the product. The activation energy, E_a for the oxidation process (α range 0.2–0.8) was found to be 122 ± 7 kJ mol^{-1}.

3.2.2. Isothermal kinetics

In order to validate the reaction mechanism and kinetic parameter obtained from non-isothermal experiments and the evaluated kinetic parameters, isothermal experiments were carried out at various temperatures.

The rate of the reaction under isothermal conditions is expressed by the following relation:

$$\frac{d\alpha}{dt} = f(\alpha)k(T) \tag{5}$$

The above equation can be expressed by its integral form as:

$$g(\alpha) = \int_0^\alpha \frac{d(\alpha)}{f(\alpha)} = \int_0^t k(T)dt \tag{6}$$

$$g(\alpha) = kt \tag{7}$$

where 'k' is temperature dependent Arrhenius rate constant and 't' is time.

After separation of variables, Eq. (6) can be rearranged into:

$$\int_0^\alpha \frac{d\alpha}{f(\alpha)} = k \int_0^{t_\alpha} dt \tag{8}$$

where 't' is the time at which the conversion fraction 'α' is reached. If we denote the primitive function of the integral at the left side of the Eq. (8) as F, we can get:

$$F(\alpha) - F(0) = kt_\alpha \tag{9}$$

$$t_\alpha = \frac{[F(\alpha) - F(0)]}{k}$$

The temperature dependence of the rate constant 'k' is expressed by Arrhenius Eq. (10).

$$k(T) = A \exp\left[\frac{-E}{RT}\right] \tag{10}$$

Combination of Eqs. (9) and (10) gives expression for the time t_α:

$$t_\alpha = \frac{1}{A_\alpha \exp(-B_\alpha/T)} \tag{11}$$

where the activation parameters A and B are given as:

$$A_\alpha = \frac{A}{[F(\alpha) - F(0)]} \tag{12}$$

$$B_\alpha = \frac{E_\alpha}{R}$$

The subscript 'α' at the A_α, B_α and t_α designates the values related to the fixed value of conversion. Hence, the parameters A_α and B_α can be obtained from a series of isothermal measurements. These parameters can be obtained by directly using Eq. (11) or from its logarithmic transformation leading to the linear dependence $\ln t_\alpha = f(1/T)$. The slope of the straight line obtained by such curves equal E_α/R as reported by Simon [21].

From the non isothermal oxidation of boron powder it is observed (Fig. 3) that the maximum gain in weight is in temperature range 700–850 K. Hence, isothermal experiments were carried

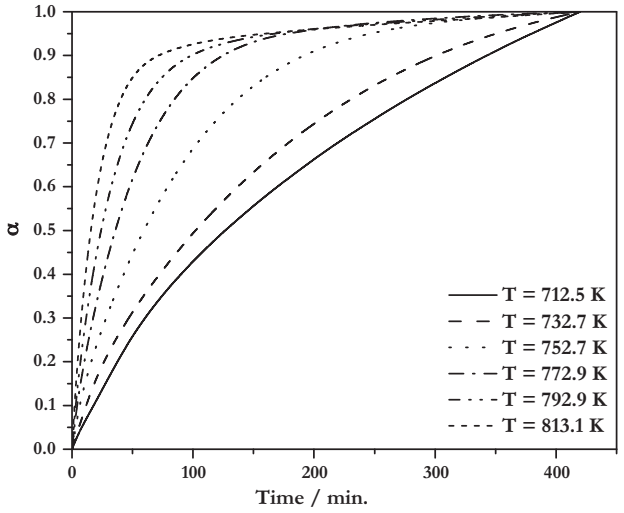

Fig. 5. A plot of fraction of oxidation α with time at various temperatures for electrodeposited boron (isothermal experiment).

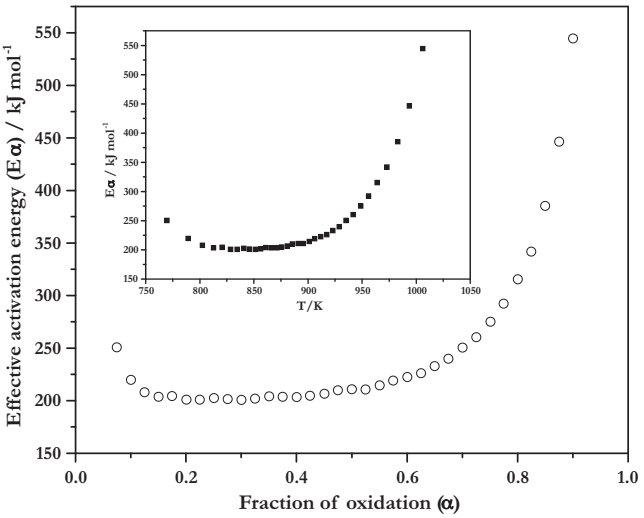

Fig. 7. A plot of E_α as a function of α for boron-commercial powder. A plot of E_α with average temperature is shown as an inset.

out at 712, 732, 752, 772, 792 and 813 K. Each isothermal experiment was carried out for 7 h as no appreciable weight change was observed beyond this time period. From the weight gain the fraction oxidized was evaluated and plotted as a function of time (Fig. 5).

The variation of effective activation energy (E_α) as a function of α is shown in Fig. 6. The E_α remains constant (for α = 0–0.8) and then decreases rapidly (for α = 0.8–1). The average value of E_α obtained for α = 0–0.8 is 102 ± 2 kJ mol^{-1}. The variation of effective activation energy (E_α) with average time is shown as an inset in Fig. 6. The E_α remains constant for certain interval of time and then it decreases rapidly. The variation is almost similar to the variation of E_α with α. The rapid decrease in the value of E_α could be due to the fact that in this region overlapping reaction mechanism (nucleation and growth) might be operating simultaneously during the oxidation.

3.3. Kinetics of oxidation of boron-commercial

The variation of percentage gain in weight of boron-commercial powder during oxidation reaction is similar to the electrodeposited boron. The observed weight gain is dependent on the rate of heating and theoretical weight gain was not attained in the temperature range and heating rate employed. A weight gain of ~88% was observed when boron powder was heated at a rate of 1 K min^{-1} while ~65% weight gain was observed when sample was heated at 15 K min^{-1}. The gain in weight is less compared to the electrodeposited boron powder. A similar behavior as reported for electrodeposited boron was observed for the variation of onset temperature with heating rate. The onset temperature for the oxidation reaction is higher compared to the electrodeposited boron. This is due to low surface area and higher particle size of the boron particles in the boron-commercial powder.

The variation of effective activation energy as a function of α is shown in Fig. 7. The variation of effective activation energy with temperature is shown as an inset in the same figure. The activation energy obtained using model-free method for boron-commercial is found to be 205 ± 7 kJ mol^{-1}.

Isothermal kinetic analysis was also carried out for boron-commercial. The variation of 'α' with time is shown in Fig. 8. The variation of 'E_α' with 'α' and average 't' is shown in Fig. 9. This shows a continuous decrease in the 'E_α' with 'α' and average 't'. The constancy of 'E_α' for 'α' = 0–0.8 as observed in case of electrodeposited boron was not observed in boron 'c'.

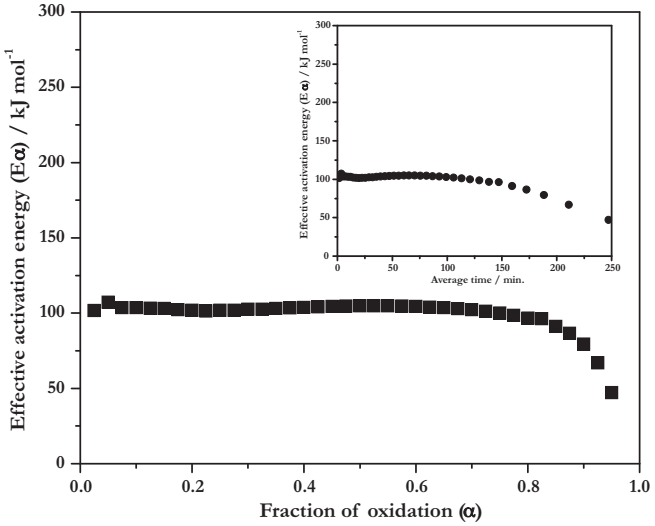

Fig. 6. A plot of E_α as a function of α for electrodeposited boron powder. A plot of E_α with average time is shown as an inset (isothermal experiment).

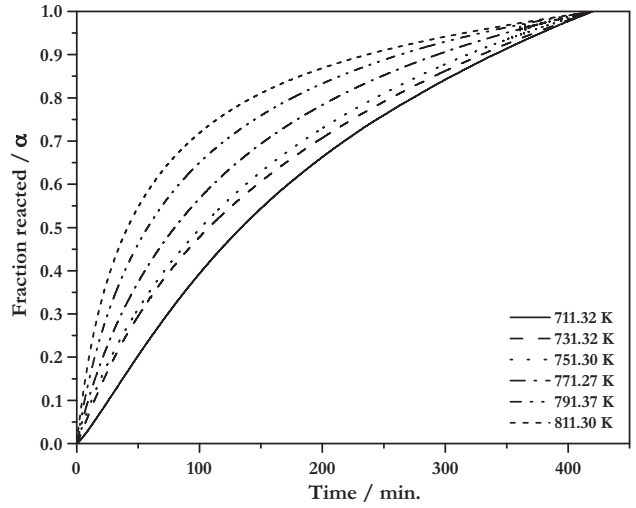

Fig. 8. A plot of fraction of oxidation α as a function of time at various temperatures for boron-commercial (isothermal experiment).

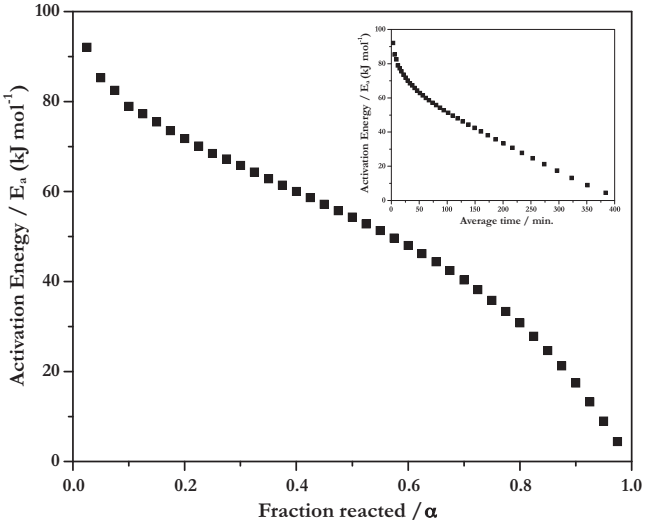

Fig. 9. Plot of E_α as a function of α for boron-commercial powder. A plot of E_α as a function of average time is shown as an inset (isothermal experiment).

The variation observed for 'E_α' with 'α' shows that electrodeposited boron and boron-commercial follow almost similar type of mechanisms of oxidation reaction. The effective activation energy obtained by isoconversional method shows that E_α of boron-commercial is higher compared to electrodeposited boron powder. The higher value of activation energy of oxidation reaction shows low reactivity of boron-commercial towards oxygen. This is also confirmed by the low % weight gain during oxidation by boron-commercial compared to electrodeposited boron. The low reactivity of boron-commercial towards oxidation is due to higher particle size and lower specific surface area as given in Table 1. Particle size plays an important role in all the surface reactions. Gas solid reaction (oxygen and boron) is highly influenced by the particle size and specific surface area of the powder. Finer particle size of the powder provides higher specific surface area and high release of surface energy during reaction with oxygen which acts as a driving force for the oxidation reaction. Higher specific surface area of the electrodeposited boron powder provides more nucleation sites and higher exposed area for the reaction with oxygen gas. The size distribution of the particle of the boron powder is shown in Fig. 10. More than 50 vol% of the particles present in the electrodeposited boron sample has sizes below 10 μm whereas for this fraction the size is 100 μm for boron-commercial. High activation energy for the oxidation of boron-commercial is due to more population of the higher size fractions in the sample.

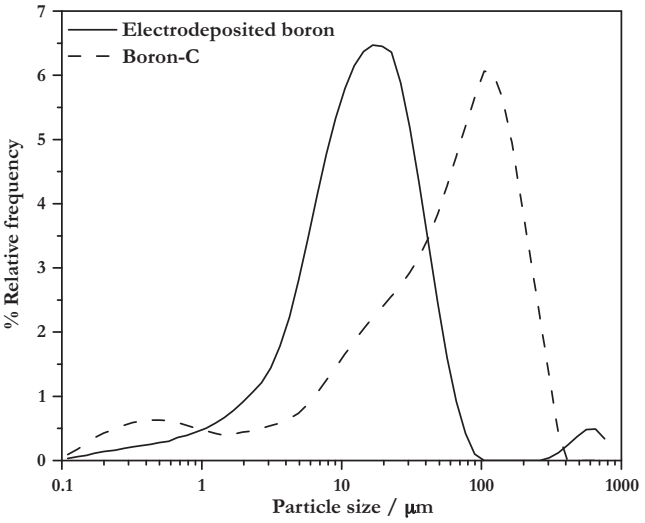

Fig. 10. Size distribution of particles in boron powder.

3.4. Mechanism of oxidation of boron powder

To get information about the reaction mechanism of the oxidation reaction we have used Coats and Redfern approximation [22]. No attempt was made to derive the activation energy using this method due to unreliable results [23]. Eq. (13) is used to identify the correct form of $g(\alpha)$ to be used for the analysis of the experimental data and to obtain the most probable reaction mechanism.

$$\ln\left[\frac{g(\alpha)}{T^2}\right] = \ln\left[\frac{AR}{E_a\beta}\left(1-\frac{2RT}{E_a}\right)\right]\left[\frac{E_a}{RT}\right] \quad (13)$$

The algebraic expressions of $g(\alpha)$ functions for the most common mechanism used in the present study are listed in Table 2 [22]. The $g(\alpha)$ function describes the mechanism of the reaction. The possible mechanism was chosen based on the best linear fit with highest correlation coefficient and low standard deviation. We have chosen different models to describe the reaction mechanism of oxidation. It was observed that no single model could describe the mechanism of the complete oxidation reaction. This shows the complex nature of the oxidation of boron. For the initial stages of oxidation the reaction is described by the second order and three dimensional diffusion controlled mechanism. This shows that both boron and oxygen take part in deciding the reaction rate. The partial pressure of the oxygen in the vicinity of the sample is also a factor for the oxidation of boron powder. Later the formation of B_2O_3 nuclei takes place which grows as the reaction progresses. For $\alpha = 0.2–0.8$, first order rate (F1) law and Avrami Erofe'ev Eq. (A2) is followed. F1 corresponds to random nucleation (one nucleus per particle) and A2 corresponds to nucleation and one dimensional growth mechanism. The 'R' value or variance obtained for F1 and A2 is ~0.99 which does not change for different heating rates, which indicates the reliability of these approximation at various heating rates. For higher value of $\alpha = 0.8–1$ the reaction follows power law and progress of the reaction is controlled by three dimensional diffusion of oxygen through the oxide layer.

To get more insight into the oxidation reaction, isothermal analysis was carried out using Eq. (7). Among the various $g(\alpha)$ functions, the linear fit with high correlation coefficient and low standard deviation was obtained for A2, A3, R2, R3, D1 and F1 mechanisms. Additional information on the mechanism of the oxidation reaction was obtained from the isothermal experiment. A2 and A3 are indicative of one and two dimensional growth of the nuclei. R2 and R3 indicate the reduction in specific surface area and volume as observed in the sample after completion of the experiment. One dimensional diffusion mechanism plays an important role in the progress of the oxidation reaction once the product layer (layer of B_2O_3) is formed on the surface of boron. At this stage the rate of oxidation is controlled by the diffusion of the oxygen gas through the layer of glassy B_2O_3 which remains impervious up to 1073 K. The one dimensional diffusion mechanism observed in this study is similar to the earlier observation of parabolic rate law made by Rizzo [4].

The mechanism presented in Table 2 indicates that the mechanism of oxidation of electrodeposited boron and boron-commercial powder are similar. The observed difference in the activation energy is due to the difference in the surface area, particle size and nature of the boron (crystalline and amorphous). As no oxidation was observed till 700 K this shows that the room temperature oxidation of electrodeposited boron is a kinetically hindered process. The kinetics of oxidation inferences that electrodeposited boron can be handled without the risk of oxidation during quenching of electrode and further processing.

Table 2
List of solid state rate equations used in the present study.

Rate controlling mechanism	$g(\alpha)$	Type of kinetics analysis	$\alpha = 0$–0.2	$\alpha = 0.2$–0.8	$\alpha = 0.8$–1
P1 power law	$\alpha^{1/n}$	Non isothermal electrodeposited boron	D3, F2	F1, A2	P1 ($n = 3$), D3, D4
A2 Avrami Erofe'ev Eq. (1)	$[-\ln(1-\alpha)]^{1/2}$	Non isothermal boron commercial	D3, F2	F1, A2	P1 ($n = 3$), D3, D4
A3 Avrami Erofe'ev Eq. (2)	$[-\ln(1-\alpha)]^{1/3}$	Isothermal electrodeposited boron	A2, A4, R2, R3, D3	A2, A3, R2, R3, D1, F1	D3
A4 Avrami Erofe'ev Eq. (3)	$[-\ln(1-\alpha)]^{1/4}$	Isothermal boron commercial	〃	A2, A3, R2, R3, D1, F1	〃
R2 contracting area	$1-(1-\alpha)^{1/2}$	'*R*' square value obtained in the linear fit	>0.99	>0.99	>0.99
R3 contracting area	$1-(1-\alpha)^{1/3}$	For rest of the models	<0.95	<0.95	<0.95
D1 one dimensional diffusion	α^2				
D2 two dimensional diffusion	$(1-\alpha)\ln(1-\alpha)+\alpha$				
D3 three dimensional diffusion, Jander	$[1-(1-\alpha)^{1/3}]^2$				
D4 three dimensional diffusion, Ginstling and Brounstein	$(1-2\alpha/3)-(1-\alpha)^{2/3}$				
F1 first order	$-\ln(1-\alpha)$				
F2 second order	$1/(1-\alpha)$				
F3 third order	$[1/(1-\alpha)]^2$				

4. Conclusion

Kinetics of oxidation of electrodeposited and boron-commercial was studied under non-isothermal and isothermal conditions. Activation energy was evaluated using model-free method. The value of activation energy obtained for electrodeposited boron is $122 \pm 7\,kJ\,mol^{-1}$ and for boron-commercial this value is $205 \pm 9\,kJ\,mol^{-1}$. The effective activation energy of oxidation of boron powder is affected by the size distribution of particles, specific surface area and nature of the powder. The oxidation of boron is complex process which involves several competing mechanisms. Among these nucleation and growth, contracting area and volume and three dimension diffusion are important. Rapid oxidation of boron starts after 700 K hence electrodeposited boron can be handled safely with out the risk of oxidation during production and processing.

References

[1] V. Rajan Babu, S. Govindarajan, S.C. Chetal, Proc. of Seminar on Inherent Engineered Safety Aspects of PFBR Design, 30 April, IGCAR, Kalpakkam, 1996.
[2] C. Subramanian, A.K. Suri, Met. Mater. Process. 16 (2004) 39–52.
[3] K.U. Nair, D.K. Bose, C.K. Gupta, Miner. Proc. Extract. Metall. Rev. 9 (1992) 283–291.
[4] H.F. Rizzo, in: G.K. Gaule, J.T. Breslin, J.R. Pastore, R.A. Shuttleworth (Eds.), Boron: Synthesis, Structure and Properties, Ist ed., Plenum Press Inc., New York, 1960, pp. 175–181.
[5] C.P. Talley, Aero Space Eng. 18 (6) (1959) 37–41.
[6] T.G. DiGiuseppe, P.J. Davidovits, J. Chem. Phys. 74 (1981) 3287–3291.
[7] I. Glassman, F.A. Williams, P. Antaki, 20th Symp (Int.) on Combust, The combustion Institute, Pittsburgh, 1984, pp. 2057–2064.
[8] C.L. Yeh, K.K. Kuo, Prog. Energy Combust. Sci. 22 (1996) 511–541.
[9] M.K. King, Combust. Sci. Technol. 5 (1972) 155–164.
[10] M.K. King, Combust Sci. Technol. 8 (1974) 255–273.
[11] M.K. King, 19th JANNAF Combst. Meet. CPIA Publication 366 (2) (1989) 27–42.
[12] M.K. King, 26th JANNAF Combst. Meet. CPIA Publication 529 (2) (1989) 203–211.
[13] A. Macek, J.M. Semple, Combust. Sci. Technol. 1 (1969) 181–191.
[14] J. Cueilleron, F. Thevenot, in: V.I. Matkovich (Ed.), Boron and Refractory Borides, Springer-Verlag, New York, 1977, pp. 207–214.
[15] A. Jain, S. Anthonysamy, K. Ananthasivan, G.S. Gupta, Thermochim. Acta 500 (2010) 63–68.
[16] A. Jain, S. Anthonysamy, C. Ghosh, R. Divakar, E. Mohandas, K. Ananthasivan, G.S. Gupta, V. Ganesan, DAE BRNS 3rd International Symposium on Materials Chemistry, 7–10 December, BARC, Mumbai, India, 2010.
[17] M.E. Brown, D. Dollimore, A.K. Galwey, Comprehensive Chemical Kinetics, vol. 22, Elsevier, Amsterdam, 1988, p. 99.
[18] A.A. Abu-Sehly, Thermochim. Acta 485 (2009) 14–19.
[19] A.A. Joraid, Thermochim. Acta 456 (2007) 1–6.
[20] S. Vyazovkin, in: M.E. Brown, P.K. Gallagher (Eds.), Hand Book of Thermal Analysis and Calorimetry: Recent Advances, Techniques and Applications, vol. 5, Elsevier B.V., 2008, pp. 503–538.
[21] P. Simon, J. Therm. Anal. Calorim. 76 (2004) 123–132.
[22] A.N. Coats, J.P. Redfern, Nature 201 (1964) 68–69.
[23] S. Vyazovkin, C.A. Wight, Thermochim. Acta 340–341 (1999) 53–68.